

Spatial Sensitivity of Capacitors in Distributed Resonators and Its Application to Fine and Wide Frequency Tuning Digital Controlled Oscillators

Win CHAIVIPAS^{†a)}, Nonmember, Kenichi OKADA[†], and Akira MATSUZAWA[†], Members

SUMMARY Analysis of resonance frequency in shorted transmission lines with inserted capacitor has been made. The analysis shows a resonance frequency dependence on capacitance position on a shorted transmission line. Two analysis methods are presented to predict the resonance frequency and understand how the inserted capacitor affects the resonance frequency of the shorted transmission line. Using this knowledge we propose a new structure for digital controlled oscillators utilizing the capacitance's sensitivity dependence on position of the shorted transmission line to increase the frequency resolution. A 9 GHz transmission line based digital controlled oscillator was designed and fabricated as a proof of concept. Measured results show that more than 100 times frequency step resolution increase is possible utilizing the same tuning capacitor size located at different points on the transmission line.

key words: digital controlled oscillators, transmission line, frequency tuning

1. Introduction

All digital phase-locked loop (ADPLL) frequency synthesizers offer several advantages over the conventional charge-pump based phase-locked loop synthesizer. In addition to greater tolerance to process, voltage and temperature (PVT), the availability of almost all intermediate signals in digital form offers the ability to perform digital signal processing on the immediate signals making possible such techniques as direct frequency modulation [1], [2], dynamic loop bandwidth control [3], and direct reference feed-forwarding method [4], [5] for fast settling. In addition, the structure of the ADPLL lends itself very well to adaptability and should therefore be a good candidate for software defined radio and cognitive radio. This leads from the fact that the operating range of the ADPLL is not limited as the traditional charge-pump based circuit in which the control voltage of the VCO is inherently limited by linear range of operation of the charge-pump or loop filter. As the ADPLL's DCO operate on input digital code, the frequency range limit is set by the number of bit resolution which can be afforded in the system.

Several design challenges, however, exist in ADPLL. One of which is the design of the digital controlled oscillator (DCO). To account for PVT variation, usually a large margin for frequency tuning should be made available. In

addition, since specifications in some standards require frequency accuracy of synthesizers in the range of tens or hundreds of kilo-hertz, fine frequency tuning steps are also necessary. For example [6] utilizes 7-bit binary resolution for PVT calibration, 64-bit unit for acquisition, 128-bit unit for tracking, and 3 bit unit for fractional tracking. This leads to more than 20 bits tunable range. Although linearity is not critical for all but several of the LSBs, achieving this level of tuning range requires capacitors of several orders of magnitude difference in value and size. Reference [7] mentions utilizing MOS varactors with as small as 50 aF in 90 nm CMOS technology to achieve the necessary size of tuning step. Switching such small capacitors will be difficult as switch and varactor biasing parasitic capacitance can easily exceed the size of the capacitor. This problem only increases with frequency of operation of the systems as the parasitics become more significant. Although signal processing methods such as high-speed delta-sigma dithering can help achieve smaller effective tuning resolution, this comes at a cost of power. For example, [1] mentions using 8-bit delta-sigma frequency dithering at 600 MHz to increase the effective resolution. If these requirements could be reduced, significant power could be saved.

This paper analyzes the resonance frequency's sensitivity to capacitors in shorted transmission lines. Analysis and measurement data shows that depending on the position of the loaded capacitor, its effect on the resonator's resonance frequency will change. More than 100 times difference in frequency step was measured using the same size capacitor on different locations of the transmission line. Based on this method, we propose a new DCO configuration allowing simultaneous wide tuning and fine frequency step control. A simple and intuitive method for estimating the resonance frequency of the capacitor loaded shorted transmission line is also proposed along with methods for the analysis and design of this new DCO.

2. Analysis of Shorted-Transmission Line with and without Shunted Input Capacitor

2.1 Analysis of Shorted Transmission Line

It is well known that transmission lines can be used as a resonator when one of its ends are left shorted or opened. In particular, the shorted transmission line is of interest since

Manuscript received October 10, 2007.

Manuscript revised December 21, 2007.

[†]The authors are with the Department of Physical Electronics, Tokyo Institute of Technology, Tokyo, 158-8552 Japan.

a) E-mail: win_chaivipas@ssc.pe.titech.ac.jp

DOI: 10.1093/ietele/e91-c.6.918

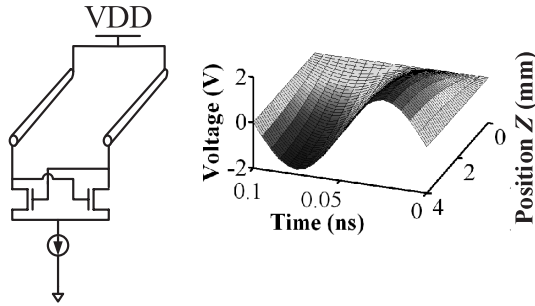


Fig. 1 Typical transmission line based resonator and voltage wave.

a $\lambda/4$ section of it will produce an anti-resonance, or parallel resonance, which can be used in place for LC tanks in cross-coupled type differential oscillators. The resulting, commonly used oscillator is shown in Fig. 1.

We now derive a simple expression for the resonance frequency of the shorted transmission line. First, note that the input impedance of a shorted transmission line of length l and propagation constant β is [8]

$$Z_{in} = jZ_0 \tan(\beta l) = jZ_0 \frac{\sin(\beta l)}{\cos(\beta l)}. \quad (1)$$

Anti-resonance occurs when the impedance is maximum, which in this case means the denominator of (1) going to zero making the input impedance approach infinity for the lossless approximation

$$\cos(\beta l) = 0. \quad (2)$$

Substituting in $\beta = \omega/v_p$ solving (2) for resonance frequency and noting that $v_p = 1/\sqrt{(\mu_0 \epsilon_0 \epsilon_r)}$ results in

$$f_0 = \frac{v_p}{4l} = \frac{1}{4l \sqrt{\mu_0 \epsilon_0 \epsilon_{reff}}}, \quad (3)$$

where v_p and ϵ_{reff} are the phase velocity and the effective relative dielectric constant respectively. Equation (3) expresses the resonance frequency as a function of variables which are either constant or vary only slightly with frequency.

At resonance, the peak voltage waveform along the shorted transmission line can be expressed as

$$V(z) = V_0^+ \mathcal{R}(e^{j(\omega t - \beta z)} - e^{j(\omega t + \beta z)}) \quad (4)$$

where $\mathcal{R}(f)$ represents the real part of 'f,' and V_0^+ represents the forward propagating voltage wave component. The maximum voltage and current waveform ($\pi/2$ apart) of an approximately $\lambda/4$ long shorted transmission line at 10 GHz is shown in Fig. 3.

2.2 Analysis of Shorted Transmission Line with Input Capacitor

Usually the capacitor is placed at the input of the transmission line as shown in Fig. 2(b). To find the resonance frequency of this circuit, the same method for finding the resonance frequency was taken as before. Following this method

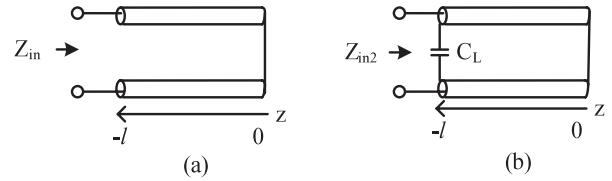


Fig. 2 Shorted transmission line (a), and shorted transmission line with input capacitor (b).

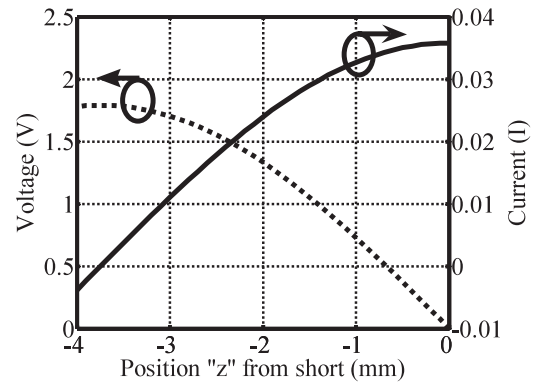


Fig. 3 Voltage amplitude of shorted transmission line.

the condition for finding the resonance frequency will be (5)

$$\cos\left(\frac{\omega}{v_p} l\right) - \omega C_L Z_0 \sin\left(\frac{\omega}{v_p} l\right) = 0 \quad (5)$$

Finding the explicit expression for ω using (5) is difficult, however if an approximation (6) is made.

$$\omega C_L Z_0 \ll 1 \quad (6)$$

then the resulting resonance frequency can be found as (7).

$$f_0 \approx \frac{1}{4(l \sqrt{\mu_0 \epsilon_0 \epsilon_{reff}} + C_L Z_0)} \quad (7)$$

$$f_0 \approx \frac{1}{4((l + C_L/C') \sqrt{\mu_0 \epsilon_0 \epsilon_{reff}})}$$

Where the relation $Z_0 = 1/(v_p * C')$ [9] was used on the second equation, and C' is the capacitance per unit length of the transmission line. Details of this derivation are given in Appendix A. Calculated values of resonance frequency is compared to simulated values using Agilent's advanced design systems (ADS) ideal transmission line model with loss in Fig. 4. Errors between simulated and calculated values are shown in Fig. 5. Two ideal transmission line models (ADS) and one coplanar waveguide characterized by a 3D electromagnetic simulator (HFSS) were used. Simulated parameters for structures used in this simulation are shown in Table 1. From Fig. 4 and Fig. 5 it is clearly seen that the accuracy of (7) is quite high for loaded capacitance under 100 fF. This is a reasonable range as it is observed in Fig. 4 that the tuning range of more than 25 percent is achieved with this value while the calculation error is well below 3% in this range.

Comparing (7) to (3) it is noted that in terms of resonance frequency, the capacitor loaded resonator can be approximated with a resonator without a loading capacitor but with a $\Delta l = C_L/C'$ length extension as shown in Fig. 6. This allows quick and intuitive estimation of the resonance frequency.

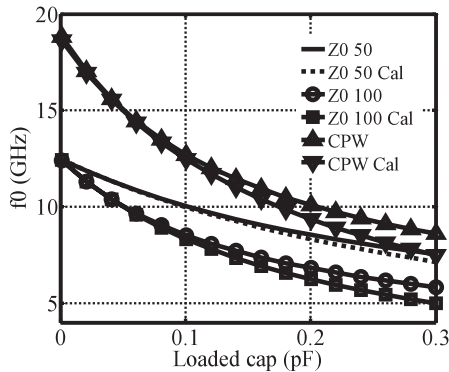


Fig. 4 Comparison between simulated and calculated resonance frequency.

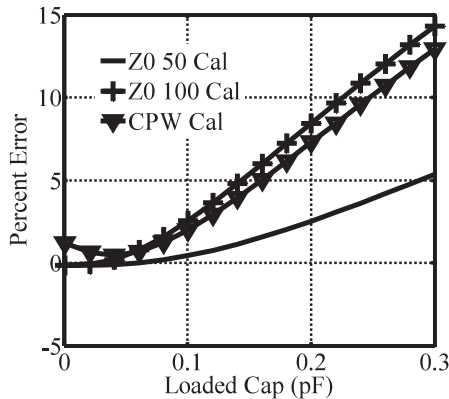


Fig. 5 Error in calculation of resonance frequency.

Table 1 Parameters for simulated transmission line components.

	model	Z0	$\epsilon_{r\text{eff}}$ @15GHz	Loss (dB/mm) @15GHz	length (μm)
Z0 50	ADS	50	4	0.147	3000
Z0 100	ADS	100	4	0.147	3000
CPW	EM	67	4.014	0.439	2000

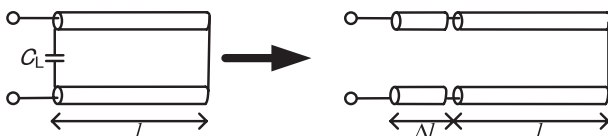


Fig. 6 Capacitance in the middle of the transmission line is reflected to an equivalent input capacitance.

3. Position Based Capacitance Sensitivity

The variation in voltage and current along the line of a short circuit transmission line seen in Fig. 3 gives a hint that the effect of a capacitance on the resonance frequency will also change with position along the line (Fig. 7).

Two pieces of information are important in analyzing the capacitance's effect on an arbitrary transmission line. First it is important to know how the capacitor placed in the transmission line affects the resonance frequency. Second it is convenient to have an expression to estimate the resonance frequency as a result of the capacitance. The second point especially is important in practice, since usually transmission lines are characterized using 3D EM simulation which takes substantial simulation time, making it usually not practical to sweep over many lengths of the transmission line. To achieve the above mentioned goals we apply two methods of analysis to the capacitor shorted transmission line.

3.1 Taylor Series Expansion

Following the same method earlier for finding the resonance frequency of the system, and with the help of Fig. 7, it can be shown that (8) must be met for resonance.

$$\cos\left(\frac{\omega l_T}{v_p} + \frac{Z_0 \omega C_L}{2}\right) + \frac{Z_0 \omega C_L}{2} \sin\left(\frac{\omega}{v_p}(l_T - 2l_1)\right) \cong 0 \quad (8)$$

Directly solving (8) will result in a very complex function. Instead we divide (8) into three conditions and apply Taylor Series Expansion on each part.

1) Capacitor Near Middle of Transmission Line

In general when the capacitor is located near the middle of the transmission line, the resonance frequency can be computed as follows.

$$f_0 \cong \frac{\frac{l_T}{v_p} + \frac{1}{2}Z_0 C_L \pm \sqrt{\left(\frac{l_T}{v_p} + \frac{1}{2}Z_0 C_L\right)^2 - \frac{\pi Z_0 C_L}{v_p}(l_T - 2l_1)}}{2\pi Z_0 C_L (l_T - 2l_1)/v_p} \quad (9)$$

In the special case when the capacitor is located exactly in the middle of the shorted transmission line

$$f_0 = \frac{1}{4} \left(\frac{1}{l_T \sqrt{\mu_0 \epsilon_0 \epsilon_r} + \frac{Z_0 C_L}{2}} \right) \quad (10)$$

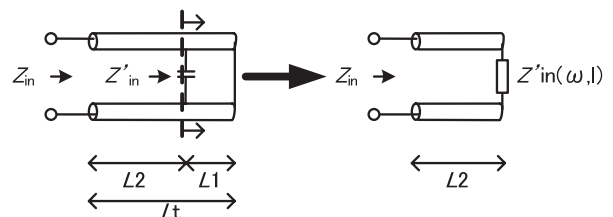


Fig. 7 Shorted transmission line with capacitance loaded at arbitrary position.

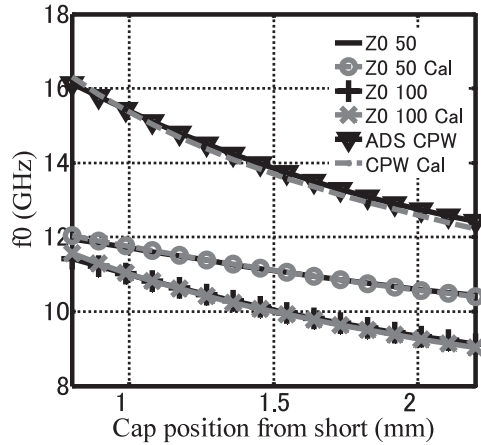


Fig. 8 Capacitor near middle of transmission line simulated and calculated resonance frequency for Taylor series estimation, total length $3000\mu\text{m}$.

Equation (10) when compared to (7) shows that a capacitor located in the middle of the shorted transmission line's effect on the resonance frequency is half as if it was at the open end. Comparison between simulated and calculated results is shown in Fig. 8, and calculation error is shown in Fig. 11 (mid section).

2) Capacitor Near Short End of Transmission Line

A transmission line with a capacitor near the short circuit end of the transmission line will, in general, have a resonance frequency described approximately by the solution to

$$\omega^3 - \frac{v_p\pi}{l_T - 2l_1}\omega^2 + v_p \left[\frac{\pi^2 Z_0 C_L v_p + 16l_T}{4Z_0 C_L (l_T - 2l_1)^2} \right] \omega - \frac{2\pi v_p^2}{Z_0 C_L (l_T - 2l_1)^2} = 0 \quad (11)$$

This can be solved by using Cardano's method for solving the general third order equation:

$$\begin{aligned} x^3 + ax^2 + bx + c &= 0 \\ x &= \frac{p}{3u} - u - \frac{a}{3} \\ p &= b - \frac{a^2}{3} \\ q &= c + \frac{2a^3 - 9ab}{27} \\ u &= \sqrt[3]{\frac{q}{2} \pm \sqrt{\frac{q^2}{4} + \frac{p^3}{27}}} \\ u_{2,3} &= u \left(-\frac{1}{2} \pm \frac{\sqrt{3}}{2} \right) \end{aligned} \quad (12)$$

Simulated and calculated comparison is shown in Fig. 9, and the calculation error in Fig. 11 (left section).

3) Capacitor Near Open End of transmission line

When the capacitor is near to the open of the transmission line the resonance frequency can be approximated with (13) which is similar to (11)

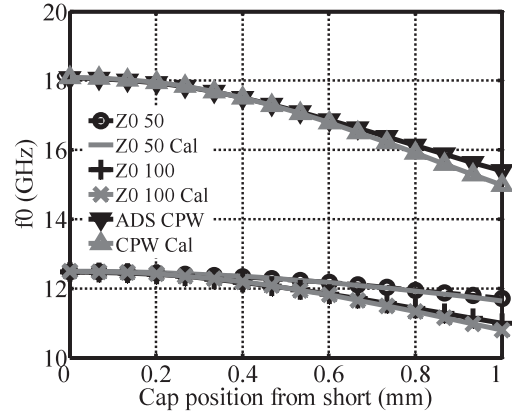


Fig. 9 Capacitor near short end simulated and calculated resonance frequency for Taylor series estimation, total length $3000\mu\text{m}$.

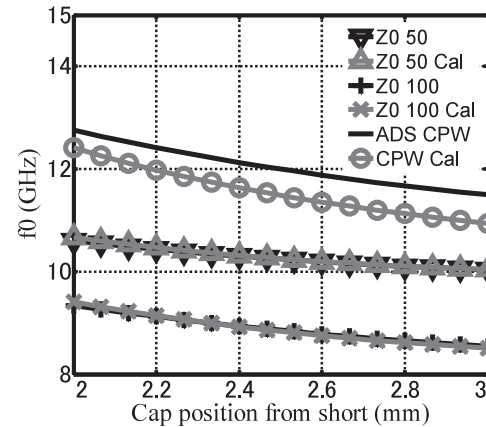


Fig. 10 Capacitor near open end simulated and calculated resonance frequency for Taylor series estimation, total length $3000\mu\text{m}$.

$$\omega^3 + \frac{v_p\pi}{l_T - 2l_1}\omega^2 + v_p \left[\frac{\pi^2 Z_0 C_L v_p - 16l_T - 16Z_0 C_L v_p}{4Z_0 C_L (l_T - 2l_1)^2} \right] \omega + \frac{2\pi v_p^2}{Z_0 C_L (l_T - 2l_1)^2} = 0 \quad (13)$$

This can be solved similarly with (11) using Cardano's method (12). Comparison between the calculated and simulated resonance frequency is shown in Fig. 10, while Fig. 11 (right section) show the error of the estimation. Details of the derivation of (8), (9), (11) and (13) can be found in Appendix B.

3.2 Equivalent Input Capacitance Method

While the Taylor series approximation serves to give a direct, and relatively accurate approximation of resonance frequency when a capacitor is inserted at certain points, the resulting approximating equations are complex and does not give a good idea of how the inserted capacitance affects the shorted transmission line intuitively. For this reason, another analysis method was devised.

This second method, which will be called the equivalent input capacitance method, models the system as fol-

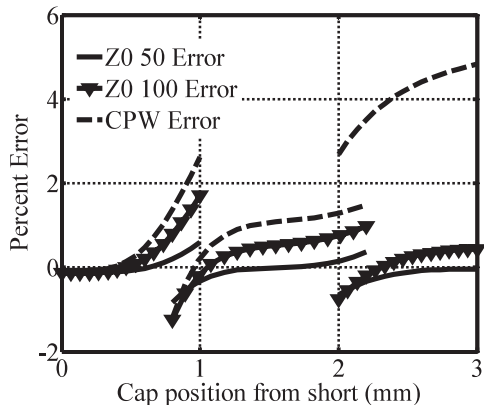


Fig. 11 Error in estimation of the resonance frequency of using Taylor Series estimation. Calculation of each section overlaps, left section is for calculation near short, middle is for when the capacitor is near mid section, right part is when the capacitor is near the open end.

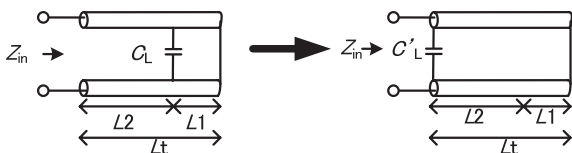


Fig. 12 Capacitance in the middle of the transmission line is reflected to an equivalent input capacitance.

lows. If the resonance frequency of a shorted transmission line with a capacitor inserted at any arbitrary location can be modeled with a shorted transmission line with a capacitor inserted at the input, how would the value of that equivalent capacitor change with the location of the inserted capacitor? The concept of this method is shown in Fig. 12. The equation governing the value of the equivalent input capacitance can be found by equating the equations governing resonance of the two circuits in Fig. 12, i.e. by comparing (5) and (8), (14) can be found. The resulting relation, shown in (14), derived in Appendix C.

$$C'_L = \frac{C_L}{2} + \left(\frac{C_L}{2}\right) \sin\left(\frac{\omega}{v_p}(2l_1)\right) \cot\left(\frac{\omega}{v_p}l_t\right) - \left(\frac{C_L}{2}\right) \cos\left(\frac{\omega}{v_p}(2l_1)\right) \quad (14)$$

Equation (14) shows that the equivalent input capacitance in terms of resonance frequency is a function of the inserted capacitance, position of the inserted capacitance from short circuit end, and frequency. This equation may seem complex at first, however, it can easily be shown; for example, if the inserted capacitance is located in the middle of the shorted transmission line, its effective value would be half of its value if it was inserted at the input of the shorted transmission line as predicted by (10).

Figure 13 plots an example of equivalent input capacitance against position of the inserted load capacitance on a shorted transmission line at 3 frequencies. It can be seen that in general, the equivalent input capacitance decreases as it nears the short circuit end, where it will effectively have no

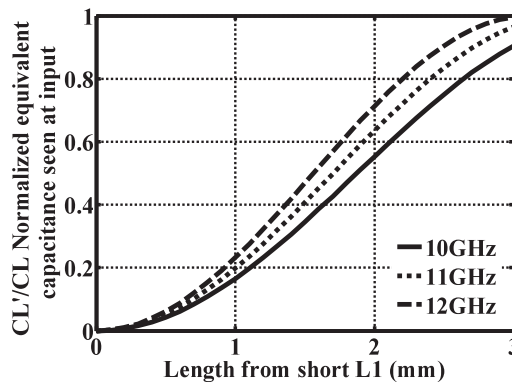


Fig. 13 Equivalent normalized reflected capacitance example, total length 3 mm.

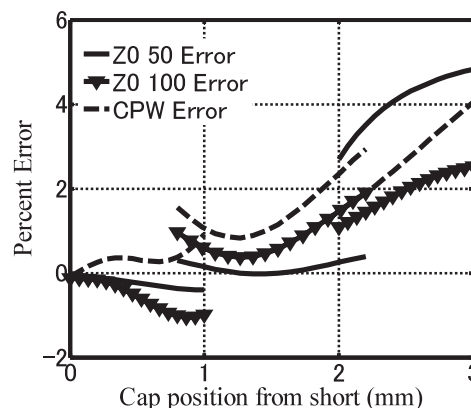


Fig. 14 Error in calculation of resonance frequency using equivalent capacitance method. Calculation of each section overlaps.

effect if it were directly on the short. For a quarter wave transmission line, the value will reach its maximum at the quarter wave length. The plot in Fig. 13 is typical of shorted transmission line with loaded capacitors and clearly shows the trend of the decrease in the effect that the loaded capacitance has on resonance frequency with respect to the position on the transmission line. In other words it can be said that the resonance frequency's sensitivity with respect to capacitance change in position decreases as the capacitor moves nearer to the short circuit end. This makes intuitive sense as the capacitor nears the short circuit end, more current will flow through the short circuit than the capacitor, making the effect of the inserted capacitor decreasing as it nears the short circuit end.

The resulting resonance frequency can be estimated with the use of (14) and (7) where the equivalent input capacitance in (14), C'_L , replaces the input capacitance in (7) C_L . Due to the fact that the equivalent input capacitance in (14) is frequency dependent, however, a few iterations may be needed to get an accurate estimate of the resonance frequency. This estimation method has similar accuracy to the Taylor method, as can be seen by comparing Fig. 11 and Fig. 14.

Both methods complement each other since the equiv-

alent input capacitance method is more intuitive, but needs an initial estimation for the resonance frequency. However, the Taylor method can directly compute the resonance frequency but is more complex. In practice, the Taylor method is used to make the initial estimation of the resonance frequency, after which subsequent adjustments are made using the equivalent input capacitance method (14), in combination with (7).

4. Utilizing Capacitance Sensitivity to Position in a DCO

With the knowledge that the capacitance’s effect on the resonance frequency greatly varies with its position on the shorted transmission line, an extra design variable becomes available to the designer. Instead of being limited with designing a capacitor bank with orders of size difference in capacitor sizes, the designer can also place the capacitor or capacitor banks at different positions on the transmission line to get a great range of tuning values. This is especially useful when fine frequency steps are needed since traditionally, getting a fine frequency step means having to deal with very small capacitor sizes. This is not always practical since the parasitics of the switch itself could easily exceed the size of the switching capacitor.

With the knowledge from the previous analysis, it is possible then to obtain very fine frequency tuning resolution by using a medium sized capacitor and placing it near to the shorted end of the transmission line. Ideally infinitesimally small frequency tuning resolution is possible by placing the capacitor closer and closer to the short circuit. The practical limit however is placed on how accurately the location of the short circuit can be determined, and how close that short circuit is to an ideal short circuit. At the same time, very coarse, large frequency tuning steps are possible for process, temperature, voltage variation calibration by placing capacitors at the open end of the shorted transmission line.

One possible realization of the new position based tuning DCO is shown in Fig. 15. Each capacitor symbol in Fig. 15 can represent either a varactor, a switch and capacitor, or a bank of these tuning varactors (capacitors).

To verify the concept of this tuning method, a DCO was designed as shown in Fig. 15. A total of eight varactors were distributed along the shorted transmission line, seven

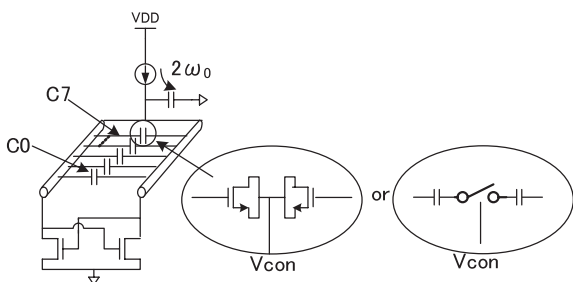


Fig. 15 Experimental prototype new DCO.

of equal size to verify that the resonant frequency change is indeed due to the position and not due to the varactor sizes. These are represented by C0 to C6 on Fig. 15. The 8th capacitor is a minimum size mos varactor placed at the same location as C6 near the shorted end of the transmission line. The chip was designed in 0.18μm CMOS process. The transmission line was designed to be coplanar strip lines (CSL). A filtering capacitor was also used to filter up-converted tail transistor noise [10].

5. Measurement

Due to the large number of control pins needed, a combination of on-chip probes, and wire-bonded signals controlled from external sources were used. While the output signals were taken from the on-chip probes, the control signals were controlled through the PCB boards wire bonded from the chip. External amplifiers and a frequency divider were also used during measurement to accommodate the limited frequency measurement range of the VCO analyzer.

To observe the effect that each capacitor has on the oscillation frequency of the system the oscillation frequency of the DCO was measured while each of the frequency tuning capacitors were turned on one by one.

The resulting measured result along with the resulting frequency step (rescaled, since the frequency was divided by 2) is plotted in Fig. 16. The oscillation frequency changed, as expected, with the position of the varactor being switched. As the position of the switched capacitor comes closer to the short circuit, the effective capacitance is smaller (Fig. 13) and so the frequency change is also smaller, as seen in Fig. 16. The maximum frequency step using the medium-sized MOS capacitor placed at the open end is 376.2 MHz. The same medium sized capacitor placed near the shorted transmission line end (150μm from the short circuit) results in a 3.45 MHz frequency step. This proves that, a frequency step difference of over 100 times can be achieved by changing the position of the capacitor alone.

The minimum size MOS capacitor placed near the shorted end showed a tuning frequency step of less than

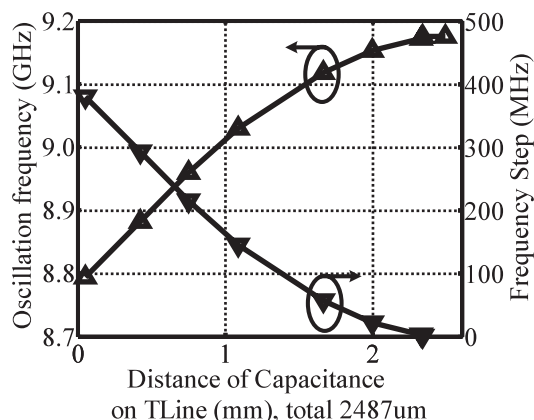


Fig. 16 Measured oscillation frequency and Frequency step VS switching position from open end.

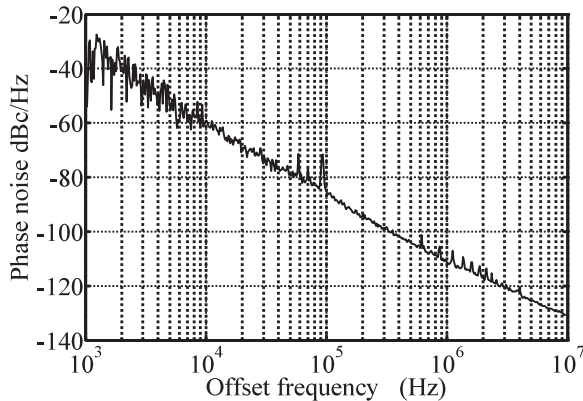


Fig. 17 Measured phase noise.

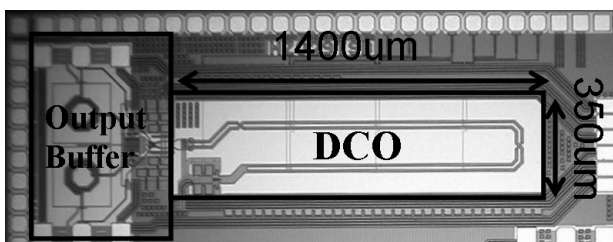


Fig. 18 Chip photo.

Table 2 Performance summary.

	[6]	This
Process	90nm	0.18um
Frequency	1.6–2.0GHz	8.79–9.17GHz
Freq. res.	12kHz @ 915MHz*	9kHz @ 910MHz**
Freq. res. limit	min MOS size	accuracy of T-Line short
Phase Noise	-149dBc/Hz@3MHz 915MHz	-125dBc/Hz@1MHz 917MHz
Power Supply	1.4V	1.8V
Current	18mA	5mA
Area	0.44mm ²	0.49mm ²
	*Minimum limit calculated	**Not minimum limited values at 900 MHz cal. from the data @ 9.17 GHz

100kHz at 9GHz. It is possible to decrease this step size even further by moving the switching capacitor nearer to the shorted transmission line.

The measured phase noise of the DCO is shown in Fig. 17. Phase noise is -105 dBc/Hz at 1 MHz offset at 9.17 GHz center frequency. This phase noise is achieved with 5 mA of bias current from a 1.8 V power supply. It is possible to improve the phase noise by shielding the CSL from the substrate and replace the large varactors with capacitors and switches.

Table 2 compares this DCO with that of [6]. First, several facts should be taken into account for a more meaningful comparison between the two systems. First, the area of the DCO in [6] includes frequency dividers and internal buffers. Second, the difference in operating frequency obviously affects the size of the resonator. Third the DCO in [6] does contain more than 20 bits of tuning capacitors, while our experimental DCO only has only several capacitors inserted mainly as the proof of concept. In a real DCO design

many more capacitors will be needed which would increase the capacitor area, while decreasing the transmission line area. Last, the high current consumption in [6] was due to the requirements for meeting the stringent GSM specifications for far-off phase noise.

The first thing to notice from Table 2 is that the frequency resolution of this system using a $0.18\mu\text{m}$ CMOS system, is better than that of the 90 nm system where much smaller MOS capacitors are available. In addition, it is noted that while the frequency resolution of the system in [6] is already at its absolute minimum, our proposed system could obtain much smaller frequency resolution than shown here by placing the tuning capacitors closer to the short circuit. The phase noise of the proposed system (calculated at 917 MHz from measurement data at 9.17 GHz assuming frequency division) can be improved, and the resonator size reduced by using slow-wave transmission line.

6. Conclusion

In this paper we have analyzed the resonance frequency of the shorted transmission line, and have found a method for estimating the resonance frequency of the shorted transmission line when loaded with a capacitor at an arbitrary location using Taylor Series expansion. In addition, a more intuitive method has also been devised to understand how the sensitivity of the capacitor changes with the location of the transmission line, making its effective value decreasing with the position nearing the short circuit.

Measured values show that more than 100 times increase of frequency tuning step resolution can be achieved by simply changing the position of the capacitor alone. This knowledge gives the designer an extra dimension in the design of the digital controlled oscillator, enabling greater flexibility in designing a wide frequency tuning range and fine frequency tuning step DCO. Due to the potential increase in tuning frequency accuracy, using this technique it may be possible that the high frequency delta-sigma dithering requirement may be reduced.

Acknowledgments

The authors would like to thank Masu Laboratory and Masu Lab members for lending of the measurement equipment and support for measurement. Special thanks to Kazuma Ohashi for measurement suggestions, and Yasuhide Kuramochi for suggestions on PCB design for measurement. This work was supported by VLSI Design and Education Center (VDEC), the University of Tokyo in collaboration with Cadence Design Systems, Inc and Agilent Technologies Japan, Ltd.

References

- [1] R.B. Staszewski, K. Muhammad, D. Leipold, C.-M. Hung, Y.-C. Ho, J.L. Wallberg, C. Fernando, K. Maggio, R. Staszewski, T. Jung, K. Jinseok, S. John, I.Y. Deng, V. Sarda, O. Moreira-Tamayo, V. Mayega, R. Katz, O. Friedman, O.E. Eliezer, E. de-Obaldia, and

- P.T. Balsara, "All-digital TX frequency synthesizer and discrete-time receiver for bluetooth radio in 130-nm CMOS," IEEE J. Solid-State Circuits, vol.39, no.12, pp.2278–2291, Dec. 2004.
- [2] R.B. Staszewski, D. Leipold, and P.T. Balsara, "Direct frequency modulation of an ADPLL for bluetooth/GSM with injection pulling elimination," IEEE Trans. Circuits Syst. II, vol.52, no.6, pp.339–343, June 2005.
- [3] R.B. Staszewski and P.T. Balsara, "All-digital PLL with ultra fast settling," IEEE Trans. Circuits Syst. II, vol.54, no.2, pp.181–185, Feb. 2007.
- [4] W. Chaivipas and A. Matsuzawa, "Analysis and design of direct reference feed-forward compensation for fast-settling all-digital phase-locked loop," IEICE Trans. Electron., vol.E90-C, no.4, pp.793–801, April 2007.
- [5] W. Chaivipas, A. Matsuzawa, and P.C. Oh., "Feed-forward compensation technique for all digital phase locked loop based synthesizers," Proc. ISCAS, pp.3209–3212, May 2006.
- [6] C. Hung, R. Staszewski, N. Varton, M. Lee, and D. Leipold, "A digitally controlled oscillator system for SAW-less transmitters in cellular handsets," IEEE J. Solid-State Circuits, vol.41, no.5, pp.1160–1170, May 2006.
- [7] R.B. Staszewski, C. Hung, N. Barton, M. Lee, and D. Leipold, "A digitally controlled oscillator in a 90 nm digital CMOS process for mobile phones," IEEE J. Solid-State Circuits, vol.40, no.11, pp.2203–2211, Nov. 2005.
- [8] W. Chaivipas, T. Ito, T. Kurashina, K. Okada, and A. Matsuzawa, "Fine and wide frequency tuning digital controlled oscillators utilizing capacitance position sensitivity in distributed resonators," Proc. ASSCC, pp.424–427, Nov. 2007.
- [9] D.M. Pozar, Microwave Engineering, 2nd ed., pp.154–155, United States of America, 1998.
- [10] E. Hegazi, H. Sjolund, and A.A. Abidi, "A filtering technique to lower LC oscillator phase noise," IEEE J. Solid-State Circuits, vol.36, no.12, pp.1921–1230, Dec. 2001.

Appendix A

Using approximation (6), (5) can be approximated as

$$\begin{aligned} \cos(\beta l + \omega C_L Z_0) &\approx 0 \\ \beta l + \omega C_L Z_0 &\approx \frac{\pi}{2}, \frac{3\pi}{2}, \dots, \frac{n\pi}{2} \end{aligned} \quad (\text{A} \cdot 1)$$

using the trigonometric approximation when Δa is small

$$\cos(a + \Delta a) \approx \cos(a) - \Delta a \cdot \sin(a).$$

The resonance frequency can then be approximated as

$$\omega_0 \approx \frac{\pi}{2} \left(\frac{v_p}{l + v_p C_L Z_0} \right) \quad (\text{A} \cdot 2)$$

for the first quarter wave, using $\beta = \omega/v_p$. Then using $v_p = 1/\sqrt{(\mu_0 \epsilon_0 \epsilon_r)}$ (A·3), (7) can be obtained

$$f_0 \approx \frac{1}{4l \sqrt{\mu_0 \epsilon_0 \epsilon_{\text{reff}}} + C_L Z_0} \quad (\text{A} \cdot 3)$$

Appendix B

Taylor approximation of resonance frequency for different sections can be found as follows. First from Fig. 7, Z'_{in} can be found as

$$Z'_{in} = jX = \frac{jZ_0 \tan(\beta l_1)}{1 - Z_0 \omega C_L \tan(\beta l_1)} \quad (\text{A} \cdot 4)$$

The total input impedance on the right figure of Fig. 7 can then be written as (A·5) by representing the input impedance of the capacitor and shorted transmission line, as a variable jX

$$\begin{aligned} Z_{in} &= Z_0 \frac{Z_L + jZ_0 \tan(\beta l_2)}{Z_0 + jZ_L \tan(\beta l_2)} \\ &= Z_0 \frac{j(X + Z_0 \tan(\beta l_2))}{Z_0 - X \tan(\beta l_2)} \end{aligned} \quad (\text{A} \cdot 5)$$

where Z_L is the equivalent load at the end of the transmission line. For parallel resonance the denominator of (A·5) should be equal to 0

$$Z_0 - X \tan(\beta l_2) = 0. \quad (\text{A} \cdot 6)$$

Replacing (A·4) into (A·6) results in

$$Z_0 - \frac{Z_0 \tan(\beta l_1) \tan(\beta l_2)}{1 - Z_0 \omega C_L \tan(\beta l_1)} = 0 \quad (\text{A} \cdot 7)$$

which simplifies to

$$1 - Z_0 \omega C_L \tan(\beta l_1) - \tan(\beta l_1) \tan(\beta(l_T - l_1)) = 0. \quad (\text{A} \cdot 8)$$

It should be noted that in deriving (A·8), the relation $l_2 = l_T - l_1$ has been used. Expanding the last tangent term and simplifying, results in

$$\begin{aligned} 1 - Z_0 \omega C_L \tan(\beta l_1) - Z_0 \omega C_L \tan^2(\beta l_1) \tan(\beta l_T) \\ + \tan^2(\beta l_1) = 0. \end{aligned} \quad (\text{A} \cdot 9)$$

These terms can be simplified to sine and cosine terms as

$$\cos(\beta l_T) - Z_0 \omega C_L \sin(\beta l_1) \cos(\beta(l_T - l_1)) = 0 \quad (\text{A} \cdot 10)$$

This can be rewritten as (A·11) using Euler's rule

$$\begin{aligned} \cos(\beta l_T) - \frac{1}{2} Z_0 \omega C_L \sin(\beta l_T) \\ - \frac{1}{2} Z_0 \omega C_L \sin(\beta(2l_1 - l_T)) = 0 \end{aligned} \quad (\text{A} \cdot 11)$$

For a relatively reasonable tuning range $(1/2) * Z_0 \omega C_L$ is small, so assuming $(1/2) * Z_0 \omega C_L \ll 1$ and noting $\sin(-x) = -\sin(x)$ yields the approximation in (8)

$$\cos\left(\beta l_T + \frac{1}{2} Z_0 \omega C_L\right) + \frac{1}{2} Z_0 \omega C_L \sin(\beta(l_T - 2l_1)) \cong 0 \quad (\text{A} \cdot 12)$$

where the approximation

$$\cos(a + \Delta a) \approx \cos(a) - \Delta a \cdot \sin(a)$$

was used. Equation (A·12) is then used as the basis of deriving (9), (11) and (13). First rearranging (A·12)

$$\cos\left(\beta l_T + \frac{1}{2} Z_0 \omega C_L\right) = -\frac{1}{2} Z_0 \omega C_L \sin(\beta(l_T - 2l_1)) \quad (\text{A} \cdot 13)$$

Note that for the case where the loading capacitance is near the middle of the shorted transmission line, i.e. $l_1 \cong l_T/2$,

(A·13) can be approximated as

$$\beta l_T + \frac{1}{2} Z_0 \omega C_L \approx \frac{\pi}{2} + \frac{1}{2} Z_0 \omega C_L \sin(\beta(l_T - 2l_1)) \quad (\text{A} \cdot 14)$$

where the above equation was derived using the Taylor approximation

$$\arccos(x) \approx \frac{\pi}{2} - x$$

Again, replacing $\beta = \omega/v_p$, and noting that $\sin(x) \approx x$ for small “ x ” and simplifying results in

$$\omega^2 \frac{Z_0 C_L (l_T - 2l_1)}{2v_p} - \omega \left(\frac{l_T}{v_p} + \frac{Z_0 C_L}{2} \right) + \frac{\pi}{2} = 0 \quad (\text{A} \cdot 15)$$

which is solved using the usual quadratic equation resulting in

$$\omega_0 = \frac{\frac{l_T}{v_p} + \frac{1}{2} Z_0 C_L \pm \sqrt{\left(\frac{l_T}{v_p} + \frac{1}{2} Z_0 C_L \right)^2 - \frac{\pi Z_0 C_L}{v_p} (l_T - 2l_1)}}{Z_0 C_L (l_T - 2l_1) / v_p} \quad (\text{A} \cdot 16)$$

which is basically (9).

To arrive at (11), start with (A·12) and note that for small values of l_1 , the argument of both the sine and cosine term in (A·12) has a value close to $\pi/2$ (βl_T is quarter wave, $(1/2) * Z_0 \omega C_L$ is small). Therefore, making the Taylor expansion on (A·12) around the $\pi/2$ point leads to

$$\begin{aligned} & \cos\left(\beta l_T + \frac{1}{2} Z_0 \omega C_L\right) \\ & \rightarrow \cos\left(\frac{\pi}{2}\right) - \sin\left(\frac{\pi}{2}\right) \left(\beta l_T + \frac{1}{2} Z_0 \omega C_L - \frac{\pi}{2}\right) \\ & = -\beta l_T - \frac{1}{2} Z_0 \omega C_L + \frac{\pi}{2} \end{aligned}$$

For the first term, and

$$\begin{aligned} & \sin(\beta(l_T - 2l_1)) \\ & \rightarrow \sin\left(\frac{\pi}{2}\right) + \cos\left(\frac{\pi}{2}\right) \left(\beta(l_T - 2l_1) - \frac{\pi}{2}\right) \\ & \quad - \frac{1}{2} \sin\left(\frac{\pi}{2}\right) \left(\beta(l_T - 2l_1) - \frac{\pi}{2}\right)^2 \\ & = 1 - \frac{1}{2} \left[\beta^2 (l_T - 2l_1)^2 - \pi \beta (l_T - 2l_1) + \frac{\pi^2}{4} \right] \end{aligned}$$

for the second term. Combining the two terms together substituting $\beta = \omega/v_p$ leads to (11)

$$\begin{aligned} & \omega^3 - \frac{v_p \pi}{l_T - 2l_1} \omega^2 + v_p \left[\frac{\pi^2 Z_0 C_L v_p + 16l_T}{4Z_0 C_L (l_T - 2l_1)^2} \right] \omega \\ & \quad - \frac{2\pi v_p^2}{Z_0 C_L (l_T - 2l_1)^2} = 0 \end{aligned} \quad (\text{A} \cdot 17)$$

Lastly, to arrive at (13) first start with (A·12). Note that for a large value of l_1 , near l_T , the value of the sine term’s argument is approximately $-\pi/2$ (βl_T is quarter wave), the cosine term remains near $\pi/2$ as in the previous derivation.

$$\sin(\beta \cdot (l_T - 2 \cdot l_1))$$

$$\begin{aligned} & \rightarrow \sin\left(-\frac{\pi}{2}\right) + \cos\left(-\frac{\pi}{2}\right) \left(\beta(l_T - 2l_1) + \frac{\pi}{2}\right) \\ & \quad - \frac{1}{2} \sin\left(-\frac{\pi}{2}\right) \left(\beta(l_T - 2l_1) + \frac{\pi}{2}\right)^2 \\ & = -1 + \frac{1}{2} \left[\beta^2 (l_T - 2l_1)^2 + \pi \beta (l_T - 2l_1) + \frac{\pi^2}{4} \right] \end{aligned}$$

Combining the sine and cosine terms and substituting $\beta = \omega/v_p$ leads to (13)

$$\begin{aligned} & \omega^3 + \frac{v_p \pi}{l_T - 2l_1} \omega^2 + \left[\frac{\pi^2 Z_0 C_L v_p - 16l_T - 16Z_0 C_L v_p}{4Z_0 C_L (l_T - 2l_1)^2} \right] v_p \omega \\ & \quad + \frac{2\pi v_p^2}{Z_0 C_L (l_T - 2l_1)^2} = 0 \end{aligned} \quad (\text{A} \cdot 18)$$

Appendix C

To find the equivalent input capacitance, in terms of resonance frequency, start with the equation used to determine the resonance frequency of an input capacitance loaded transmission line (5), and the equation used to determine the frequency of the shorted transmission line with a capacitor loaded at any arbitrary location (A·11), with $\beta = \omega/v_p$, both repeated here for convenience.

$$\cos\left(\frac{\omega}{v_p} l\right) - \omega C'_L Z_0 \sin\left(\frac{\omega}{v_p} l\right) = 0 \quad (\text{A} \cdot 19)$$

and

$$\begin{aligned} & \cos\left(\frac{\omega}{v_p} l_T\right) - \frac{1}{2} Z_0 \omega C_L \sin\left(\frac{\omega}{v_p} l_T\right) \\ & \quad - \frac{1}{2} Z_0 \omega C_L \sin\left(\frac{\omega}{v_p} (2l_1 - l_T)\right) = 0 \end{aligned} \quad (\text{A} \cdot 20)$$

Note that l in (A·19) is equivalent to l_T in (A·20). Comparing (A·19) and (A·20) we solve simultaneously the second part of (A·19) to the second and third part of (A·20) to find a value of C'_L , as compared to C_L , which is necessary to make (A·19) identical to (A·20) as (A·21), or (14)

$$\begin{aligned} C'_L & = \frac{C_L}{2} + \left(\frac{C_L}{2}\right) \sin\left(\frac{\omega}{v_p} (2l_1)\right) \cot\left(\frac{\omega}{v_p} l_T\right) \\ & \quad - \left(\frac{C_L}{2}\right) \cos\left(\frac{\omega}{v_p} (2l_1)\right) \end{aligned} \quad (\text{A} \cdot 21)$$

Note that the analysis intentionally compares the equations that determine the resonance frequency as it is easier to solve than the case of the impedance making the equivalent capacitance value valid only in terms of the resonance frequency, not the impedance.



Win Chaivipas received the B.S. in Electrical Engineering from Sirindhorn International Institute of Technology Pathumthani Thailand and M.S. from Royal Institute of Technology Stockholm, Sweden in 2001 and 2003 respectively. He was an intern at National Electronics and Computer Technology Center, Thailand, where he studied DSPs and at Fujikura Ltd. Chiba, where he studied about manufacturing of flexible printed circuits and flip-chip bonding in during the summer of 2000. In 2003 he

conducted research concerning automatic tuning of RF active filters at the Swedish Institute of Microelectronics and Optics Acreo, and was a research assistant at Sirindhorn International Institute of Technology in 2004. He is currently perusing his PhD at Tokyo Institute of Technology, Tokyo, Japan.



Kenichi Okada received the B.E., M.E. and Ph.D. degrees in Communications and Computer Engineering from Kyoto University, Kyoto, Japan, in 1998, 2000, and 2003, respectively. From 2000 to 2003, he was a Research Fellow of the Japan Society for the Promotion of Science in Kyoto University. From 2003 to 2007, he worked as an Assistant Professor at Precision and Intelligence Laboratory, Tokyo Institute of Technology, Yokohama, Japan. Since 2007, he has been an Associate Professor

at Department of Physical Electronics, Tokyo Institute of Technology, Tokyo, Japan. He is a member of IEEE, the Information Processing Society of Japan (IPJSJ), and the Japan Society of Applied Physics (JSAP).



Akira Matsuzawa received B.S., M.S., and Ph.D. degrees in electronics engineering from Tohoku University, Sendai, Japan, in 1976, 1978, and 1997 respectively. In 1978, he joined Matsushita Electric Industrial Co., Ltd. Since then, he has been working on research and development of analog and Mixed Signal LSI technologies; ultra-high speed ADCs, intelligent CMOS sensors, RF CMOS circuits, digital read-channel technologies for DVD systems, ultra-high speed interface technologies for metal and

optical fibers, a boundary scan technology, and CAD technology. He was also responsible for the development of low power LSI technology, ASIC libraries, analog CMOS devices, SOI devices. From 1997 to 2003, he was a general manager in advanced LSI technology development center. On April 2003, he joined Tokyo Institute of Technology and he is a professor on physical electronics. Currently he is researching in mixed signal technologies; CMOS wireless transceiver, RF CMOS circuit design for SDR, and high speed data converters. He served the guest editor in chief for special issue on analog LSI technology of IEICE transactions on electronics in 1992, 1997, and 2003, the vice-program chairman for International Conference on Solid State Devices and Materials (SSDM) in 1999 and 2000, the Co-Chairman for Low Power Electronics Workshop in 1995, a program committee member for analog technology in ISSCC and the guest editor for special issues of IEEE Transactions on Electron Devices. Now he serves the chairman of Silicon Analog and RF committee, the vice chairman of Integrated Circuit and Devices on IEICE, the vice chairman of 177 committee on JSPS, IEEE SSCS elected Adcom and IEEE SSCS Distinguished lecturer. He received the IR100 award in 1983, the R&D100 award and the remarkable invention award in 1994, and the ISSCC evening panel award in 2003 and 2005. He is an IEEE Fellow since 2002.